

Impact essential work of fracture toughness of ABS/polyamide-6 blends compatibilized with olefin based copolymers

Guralp Ozkoc · Goknur Bayram · Erdal Bayramli

Received: 21 August 2007 / Accepted: 18 January 2008 / Published online: 19 February 2008
© Springer Science+Business Media, LLC 2008

Abstract The impact fracture toughness of acrylonitrile-styrene-butadiene/polyamide-6 (ABS/PA6) blends compatibilized with 5% by weight carbon monoxide modified ethylene-*n* butyl acrylate-maleic anhydride (EnBACO-MAH) or ethylene-methyl acrylate-glycidyl methacrylate (EMA-GMA) copolymers were examined as a function of blend ratio by standard Charpy tests, Essential Work of Fracture (EWF) Methodology and fracture surface morphologies. The samples were first processed in twin-screw extruder and they were subsequently injection moulded. The incompatibilized blends and neat-PA6 fractured in brittle manner, whereas compatibilized blends fractured in ductile manner. The EWF values yielded a maximum when weight percentages of ABS and PA6 were equal to each other. The values obtained in the case of EnBACO-MAH were higher than that of EMA-GMA regardless of blend composition in EWF tests. The trend of impact strengths observed in standard notched Charpy impact tests was in accordance with that of EWF values of blends. The

morphology of the ABS/PA6 blends exhibited differences as a function of the component ratio and compatibilizer type. These differences in topology of the fracture surfaces of the blends were utilized to understand the deformation mechanism, and to correlate the fracture toughness values of the blends.

Introduction

Blends of acrylonitrile-styrene-butadiene (ABS) with polyamide-6 (PA6) have been of commercial and scientific interest, since they combine solvent resistance, high stiffness and strength of PA6, and good toughness and surface texture of ABS with appropriate compatibilization [1–13]. Functionalized copolymers which are capable of reacting with end groups of PA6, i.e. amine or acid, and miscible with the SAN phase of ABS were utilized to compatibilize these two incompatible polymers. This route was successfully applied to obtain super-tough polymer blends [1–13].

The toughness of the materials is generally characterized by standard impact tests, such as notched/unnotched Izod or Charpy testing according to relevant standard methods. These tests are practical and industry friendly. The results obtained from these tests are comparable to each other and they do not require any complicated experimental systems. However, the fracture energies obtained by these tests are not a material property and depend on various parameters, such as material dimensions, crack geometry and rate of deformation. Moreover, they provide limited information about the fracture behaviour of ductile materials under stress in the presence of a crack [14].

There is a tendency towards the use of methods of fracture mechanics especially developed for metals to

G. Ozkoc
Department of Polymer Science and Technology, Middle East Technical University, Inonu Bulvarı, 06531 Ankara, Turkey

G. Bayram (✉)
Department of Chemical Engineering, Middle East Technical University, Inonu Bulvarı, 06531 Ankara, Turkey
e-mail: gbayram@metu.edu.tr

E. Bayramli
Department of Chemistry, Middle East Technical University, Inonu Bulvarı, 06531 Ankara, Turkey

Present Address:
G. Ozkoc
Department of Chemical Engineering, Kocaeli University Engineering Faculty, 41040 Kocaeli, Turkey

characterize the fracture behaviour and fracture toughness of polymers, polymer composites and blends. The techniques offered by linear elastic fracture mechanics (LEFM) can be utilized for better characterization of these properties, if the condition is well suited. The condition states that the test sample must be in a state of plane strain which generally occurs in very thick samples. This is difficult to obtain with conventional injection-moulding process to satisfy the small scale yielding criterion [15, 16]. Recently, *J*-integral method has been proposed to characterize ductile polymeric materials in which plane-strain toughness value can be obtained at relatively low thickness with respect to LEFM [16, 17]. However, this method requires more sophisticated equipments to measure precisely the crack propagation at very slow rate of deformations.

In this study, it is aimed to investigate the impact fracture behaviour of compatibilized ABS/PA6 blends implementing fracture mechanics rules into Charpy impact tests as a function of ABS to PA6 ratio and compatibilizer type. As an alternative to the literature, the experiments conducted in our laboratory showed that epoxydized or maleated methyl acrylate or butyl acrylate grafted polyethylene yields stable and well-dispersed phase morphology, consequently improved impact strength [18, 19].

Background information

Essential Work of Fracture (EWF) methodology was developed to characterize the fracture toughness of ductile polymers and tough composites in a practical manner. According to this technique, the energy to break a sample is partitioned into an essential work done in the fracture zone to create new surfaces and a non-essential work done in the outer plastic zone [15–17, 20–22]. The total fracture energy, W_f , can be written as follows:

$$W_f = W_p + W_e \tag{1}$$

where the essential work, W_e , is surface related and the non-essential, W_p , is volume related. Equation 1 can be expressed in terms of specific energies:

$$W_f = w_e \ell t + w_p \beta \ell^2 t \tag{2}$$

where w_e and w_p are specific essential work (energy/area) and specific non-essential work (energy/volume), respectively, and ℓ is ligament length, t is sample thickness and β is shape factor of plastic zone. A typical sample for EWF analysis is shown in Fig. 1. Normalizing Equation (2) by (ℓt) results in:

$$w_f = w_e + w_p \beta \ell \tag{3}$$

where w_f is the specific total work of fracture (energy/area). When the specific fracture energy of a material is obtained for different ligament lengths, according to Eq. 3, plots of w_f versus ℓ yield a straight line with slope of $w_p \beta$ and intercept of w_e . The specific essential work term is a material constant.

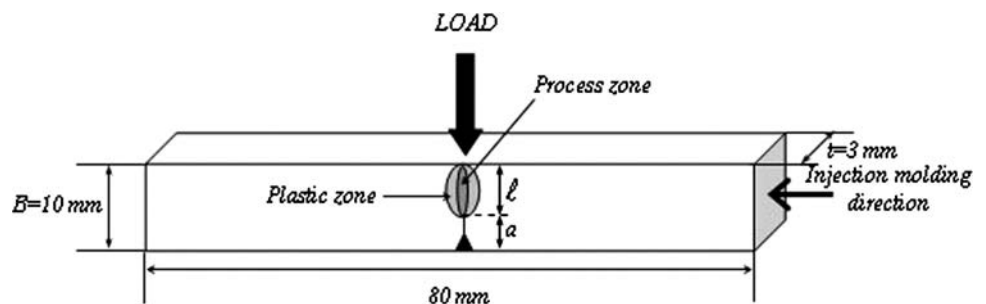
The recently established protocol states several important criteria that must be satisfied in order to apply the EWF methodology to evaluate fracture toughness [23]. They are summarized as follows:

- (i) The specimen ligament must fully yield prior to fracture initiation.
- (ii) The specimen ligament must be proportional to essential work performed in the process zone.
- (iii) Size of the outer fracture zone surrounding the fracture ligament must scale with the square of the ligament length.

In addition to the above criteria, the EWF methodology cannot be applied if the two halves of the specimen are not separated after testing [23]. When these conditions are satisfied, it is valid to apply the EWF methodology which consists of testing specimens with different ligament lengths (ℓ), measuring the area under the force versus deformation curve to obtain fracture energy (W_f), plotting specific fracture energy (w_f) versus ligament length (ℓ) and evaluating the best linear line performing regression.

The test method to determine the essential work of fracture of ductile polymers was used by many researchers and was incorporated in the European Structural Integrity Society (ESIS) Test Protocol for EWF under quasi-static loading conditions [23, 24]. However, once this concept

Fig. 1 Specimen geometry for the impact essential work of fracture method (a is the notch length and ℓ is the ligament length)



was extended to impact loading conditions, great attention was paid to this method due to its simplicity and useful information that was drawn out to understand fracture behaviour of polymers, polymer blends and composites under high rate of deformations [14, 17, 24].

The concept of EWF methodology was supported by many studies [15, 25–27]. The main difference in these approaches is the interpretation of terms, loading rate and mode, and sample geometries. Recently Kudva et al. [28] used a different nomenclature, which was analogous to Eq. 3, since the yielding criterion was not fully established in their system. The expression was written as:

$$\frac{U}{A} = u_o + u_d \ell \quad (4)$$

where U/A was total fracture energy per unit area, ℓ was the ligament length, u_o was the limiting specific fracture energy and u_d was the dissipative energy density. These should be considered as phenomenological parameters where, in certain cases, $u_o = w_e$ and $u_d = \beta w_p$.

Experimental

Materials and processing

The materials used in this study are specified in Table 1. Prior to blending, ABS and PA6 pellets were dried in vacuum at 80 °C for 12 h, ethylene-methylacrylate-glycidyl methacrylate terpolymer (EMA-GMA) and carbonmonoxide modified ethylene-*n* butyl acrylate-maleic anhydride (EnBACO-MAH) were dried at 50 °C for 4 h. The ABS/PA6 ratios were 0/100, 20/80, 50/50, 80/20 and 100/0. The ABS/PA6 part was (100-*x*)% of the blend, where *x* is the compatibilizer weight percent in the blend which varied as 0

and 5. The samples were named in the order of ABS/PA6/Compatibilizer by indicating their relative ratios.

ABS/PA6/Compatibilizer batches at pre-arranged compositions were dry-mixed first, then processed in a co-rotating twin-screw extruder (Thermoprism TSE 16 TC, L/D = 24) at a screw speed of 200 rpm and a barrel temperature profile of 190–230–230–235–240 °C. The extrudate was water cooled and chopped into small pellets. The produced pellets were again vacuum-dried at 80 °C for 12 h prior to injection-moulding. The specimens for impact fracture tests were moulded by using a laboratory scale injection-moulding machine (DSM Xplore 12 ml injection moulding machine) at a barrel temperature of 230 °C and mould temperature of 80 °C. All the injected moulded samples were kept in plastic bags at least 24 h prior to testing.

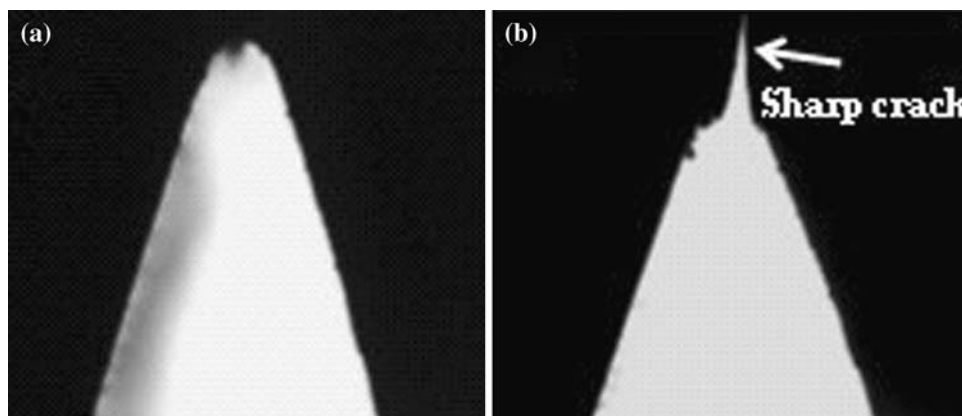
Impact essential work of fracture

The notches were first made on the injection-moulded samples by forming a slot with a notcher equipped with a V-shaped knife, and then they were sharpened by tapping a fresh razor blade into the root of the notch. Figure 1 illustrates the details of sample geometry, and Fig. 2 shows optical micrographs of the notch before and after notch sharpening. The exact notch lengths were measured under an optical microscope. In order to obtain total work of fracture energy, samples were tested with a pendulum-type Charpy impact tester (Resil Impactor, Ceast) equipped with an instrumented hammer to measure the force versus displacement during the test. The test speed was 3.5 m/s and the average ambient temperature was 25 °C. By the help of a data acquisition system (DAS 16000, Ceast), the force versus displacement curves and total fracture energies were obtained.

Table 1 Specifications of the materials used in the study

Material	Trade name and supplier	Specifications
ABS	Lustran ABS M203FC, Lanxess	Density: 1.05 g/cm ³ MFI (220 °C and 10 kg): 32.5 g/10 min Standard impact strength, easy flowing
PA6	Teklamid 6, Polyone	Density: 1.13 g/cm ³ MFI (235 °C and 2.16 kg): 34.25 g/10 min Natural, unfilled, extrusion grade
EMA-GMA	Lotader 8900, Arkema	MFI (190 °C, 2.16 kg): 6 g/10 min Melting point: 65 °C GMA content: 8 wt%
EnBACO-MAH	Fusabond A MG423D, Dupont	MFI (190 °C, 2.16 kg): 8 g/10 min Melting point: 62 °C MAH content ~1 wt%

Fig. 2 Optical micrographs of (a) Notch without pre-crack and (b) Notch with pre-crack



Charpy impact tests

The notched Charpy impact tests were performed according to ASTM D 256 using samples of 3 mm × 10 mm × 80 mm. Five samples were tested and average values were reported.

Scanning electron microscopy (SEM)

The impact-fractured sample surfaces were analysed by using a low-voltage scanning electron microscope (JEOL JSM-6400) to observe the morphologies of the blends. To prevent arching, samples were coated with a thin layer of gold.

Results and discussion

The fracture energy data revealed from standard Izod and Charpy impact tests are sum of the any kind of energy which can be absorbed during test. Despite their simplicity and convenience, they do not provide any general representation of the toughness of the samples. Since the notches are not sharp enough in standard tests, some ductile polymers do not completely break into two halves at the end of the test, which results in an incomplete fracture. In such cases, EWF concept can be utilized as an effective method for the determination of fracture toughness of ductile polymers having sharp cracks deformed at high rates.

During EWF testing, all the samples were broken into two halves except 20ABS/80PA6/5Comp. blend system regardless of compatibilizer type. In these compositions, a thin film formed as skin-layer hindered specimens to completely part into two. Thus, the impact energy measured also included the toss energy (work done to throw the sample) of these samples. However, it was thought that the toss energy (~ 0.01 J) was very small compared to overall energy, therefore it was neglected.

In order to check if the yielding criterion was satisfied, the impact test was stopped just after the hammer stroke to the specimen. Visual inspection of the specimen indicated that crack propagated before the completion of the fully yielding of the ligament. A representative photograph of one of the specimens is shown in Fig. 3. This means that criterion was not satisfied. However, even in the presence of dissatisfaction in yielding criterion of EWF, Paul and co-workers demonstrated applicability of EWF methodology using a different notation given in Eq. 4 [28].

The geometry of the stress-whitened zone formed during impact fracture testing must be investigated, since Mai and co-workers noted that in order to achieve a linear relationship between the specific fracture energy and ligament length, the volume of the stress-whitened zone must scale with the square of the ligament length [23, 29]. To check the satisfaction of this criterion, the geometry of stress-whitened zones formed after testing was visually inspected during experimentation. It was seen that the geometry is an elliptical cylinder (a cylinder whose base is an ellipse), as

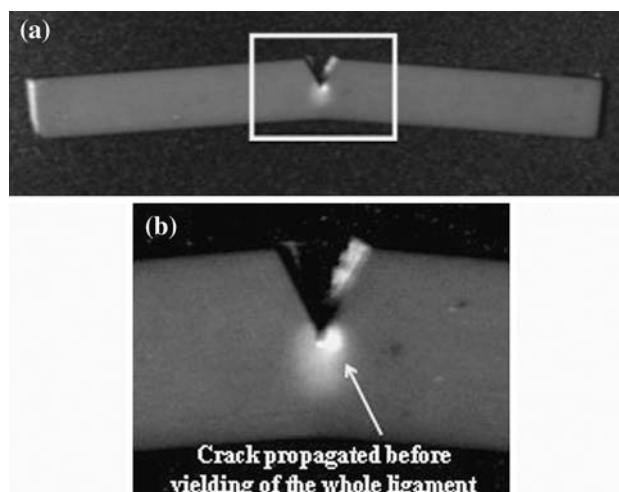


Fig. 3 Representative image of deformation of the specimen after impact test had stopped just after the hammer stroke

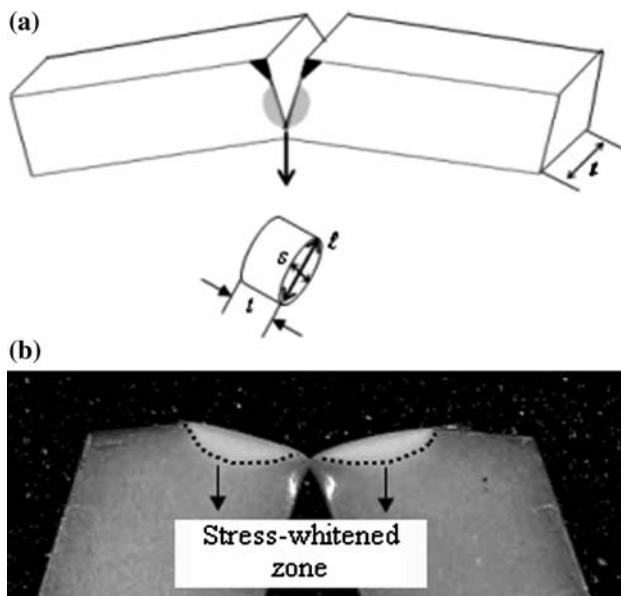


Fig. 4 Illustration of geometry of stress-whitened zone (a) Schematically (b) A real sample

schematically illustrated in Fig. 4a and b. The volume of such an elliptical cylinder body is given as follows:

$$V = \frac{\pi}{2} s l t = \beta \ell^2 t \quad (5)$$

where s and ℓ correspond to radii of ellipse, and $\beta = (\pi/2)(s/\ell)$ is a constant [28]. Here this demonstrates mathematically and geometrically that the volume of the stress-whitened zone, V , is proportional to square of the ligament length, ℓ^2 .

Figure 5a–c shows representative impact load–displacement curves for blend system of 50ABS/50PA6 compatibilized with 5% EnBACO-MAH and EMA-GMA, and incompatibilized 50ABS/50PA6. The maximum force values measured during EWF tests are nearly the same; however, for blend system of 50ABS/50PA6/5EnBACO-MAH, the area under the curve prior to maximum force and after maximum force is much higher than that of 50ABS/50PA6/5EMA-GMA indicating that crack propagation is slow with higher energy absorption associated with toughness. This kind of behaviour is typical for ductile materials [29]. In direct contradiction, incompatibilized blends of 50ABS/50PA6 exhibits a load peak, and then the load sharply drops to zero indicating fast crack propagation without any energy absorption. This type of load versus displacement characteristic indicates brittle failure [29].

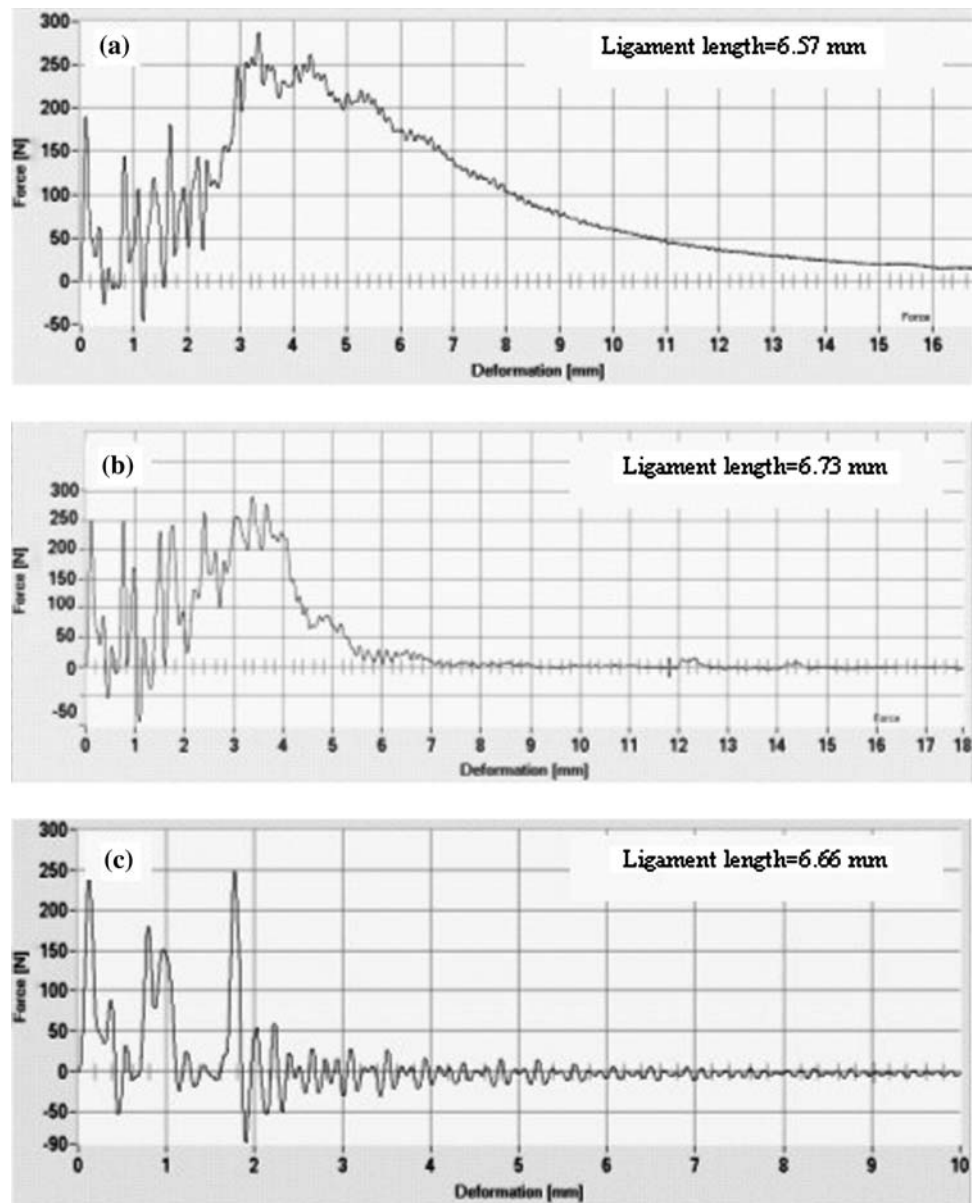
According to EWF methodology, the slopes of plots of total specific fracture energy versus ligament length are regarded as a measure of energy-absorbing process that occurs far away from the fracture surface, i.e. non-essential work in plastic zone. Figure 6a–c shows the plots of specific total impact energy versus ligament length for

ABS/PA6/Compatibilizer ternary blends. The incompatibilized blends of ABS/PA6 and neat-PA6 exhibits brittle behaviour without showing any slope which is associated with non-essential energy term. As a result of that, no stress whitening is observed for PA6 (see Fig. 7). On the other hand, ABS shows ductile fracture with a positive slope indicating energy absorption in the outer plastic zone due to the presence of rubbery phase [24, 30] with considerable stress whitening as seen from Fig. 7. Regardless of compatibilizer type and blend composition, the ABS/PA6/Compatibilizer ternary blends fractures in a ductile manner with steep positive slope indicating non-essential work done in the outer plastic zone. The good linear regression lines seen in ABS, PA6 and incompatibilized blends are distorted, and the data scattered considerably in the impact energy versus ligament length plots of compatibilized blends (see Fig. 6b and c). The photographs of specimens fractured in EWF testing show evident stress whitening as can be observed from Fig. 7.

The results of impact EWF testing are shown in Table 2 as a function of blend composition and compatibilizer type. The procedure followed to obtain dispersed particle size is described elsewhere [18]. The phase morphologies of the blends show variations with respect to composition. The incompatibilized blends exhibit dispersed particle morphology regardless of composition. For incompatibilized 80ABS/20PA6 and 50ABS/50PA6 blends, ABS is continuous, on the other hand for 20ABS/80PA6, PA6 is continuous phase. Incorporation of compatibilizer alters the morphology of 50ABS/50PA6 blends from dispersed to co-continuous. The details about morphology can be found in our recent publications [18]. Figure 8 shows the w_e and βw_p versus PA6 content for ABS/PA6/Compatibilizer blends. As can be seen, essential work increases with increasing PA6 content by giving a maximum at 50ABS/50PA6/5Comp., then it decreases for both the compatibilizers; on the other hand, non-essential term slightly increases at 50ABS/50PA6/5Comp., regardless of compatibilizer type. When two compatibilizers are compared, both essential and non-essential terms are higher in EnBACO-MAH than in EMA-GMA. It should be noted that the dispersed particle sizes are much smaller in EnBACO-MAH than those of EMA-GMA, as can be seen from Table 2. The study conducted by Huang and Paul showed that at a given rubber content, maxima are observed in both essential and non-essential terms (limiting and dissipative part, respectively). Beyond these maxima, further increase in rubber particle size reduces the essential and non-essential terms [31]. This phenomenon is also previously demonstrated elsewhere [32, 33].

The standard Charpy impact test results show similar trends in EWF depending on PA6 content (see Table 2). Strength of the materials increases with PA6 content up to

Fig. 5 Force versus displacement for (a) 50ABS/50PA6/5EnBACO-MAH (b) 50ABS/50PA6/5EMA-GMA (c) 50ABS/50PA6

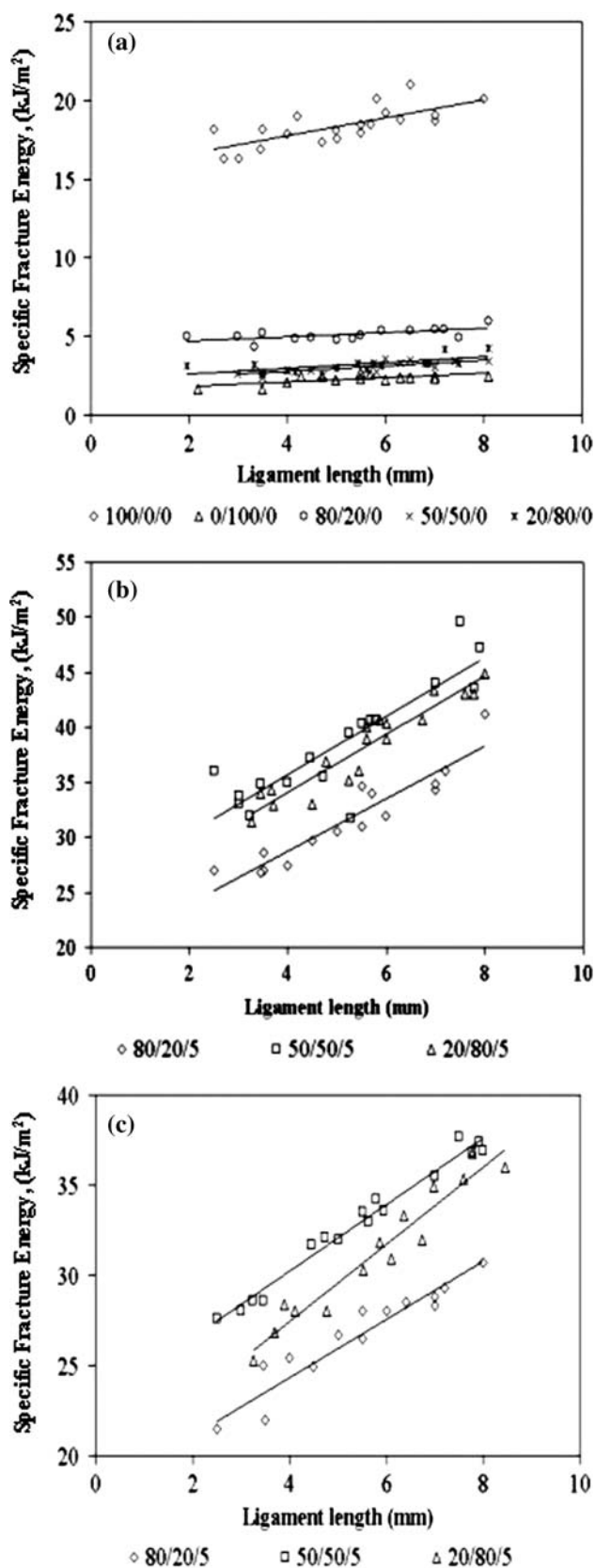


50ABS/50PA6/5Comp. blend, beyond that point it decreases. When the fracture energy values obtained in standard impact tests are compared with EWF test values, even in the highest ligament lengths, the values of EWF are lower than fracture energies obtained from standard impact test. This may account for the fact that the testing conditions in EWF are severe due to much sharper notches.

The difference in EWF parameters, i.e. essential and non-essential terms as the function of blend composition stem from difference in deformation mechanisms for PA6, ABS, incompatibilized binary ABS/PA6 blends and compatibilized ternary ABS/PA6/Compatibilizer. Neat-PA6 exhibits ductile behaviour without a notch. Once a sharp notch is introduced, due to the preclusion of shear yielding by the stress ahead of the crack tip, PA6 fails in brittle

manner [34]. On the other hand, the studies conducted on ABS have shown that the macroscopic specimens tend to fail by a combination of shear yielding and crazing of SAN matrix [35–37]. However, the microscopic combination of ABS and PA6, of course, was different from neat-materials.

For rubber-toughened semi-ductile polymers, cavitation of the rubber particles ahead of the crack may release the stresses; as a consequence shear yielding of matrix material results in a ductile failure of the material [34]. Lazzeri and Bucknall showed that fractured specimens of rubber-toughened polyamides had lines of cavitated rubber particles separated by shear yielded polyamide ligaments and referred to these features as ‘dilatational bands’ [14, 38]. Similar observation was also reported by Sue et al. for



◀ **Fig. 6** Specific fracture energy versus ligament length for (a) Pure ABS, PA6 and uncompatibilized blends, (b) Blends compatibilized with EnBACO-MAH and (c) Blends compatibilized with EMA-GMA (The numbers correspond to ABS/PA6/Compatibilizer ratios)

rubber-toughened epoxy. They called these arrays of cavitated rubber particles ‘croids’ [39]. Laura et al. [40] and Huang and Paul [31] have recently observed similar deformation in rubber-toughened polyamides. The particle size also has a crucial importance in the toughening mechanism. The crazes are initiated in rubber-toughened materials by large particles at equatorial sites where stress concentration is maximum, sometimes subsequently rubber

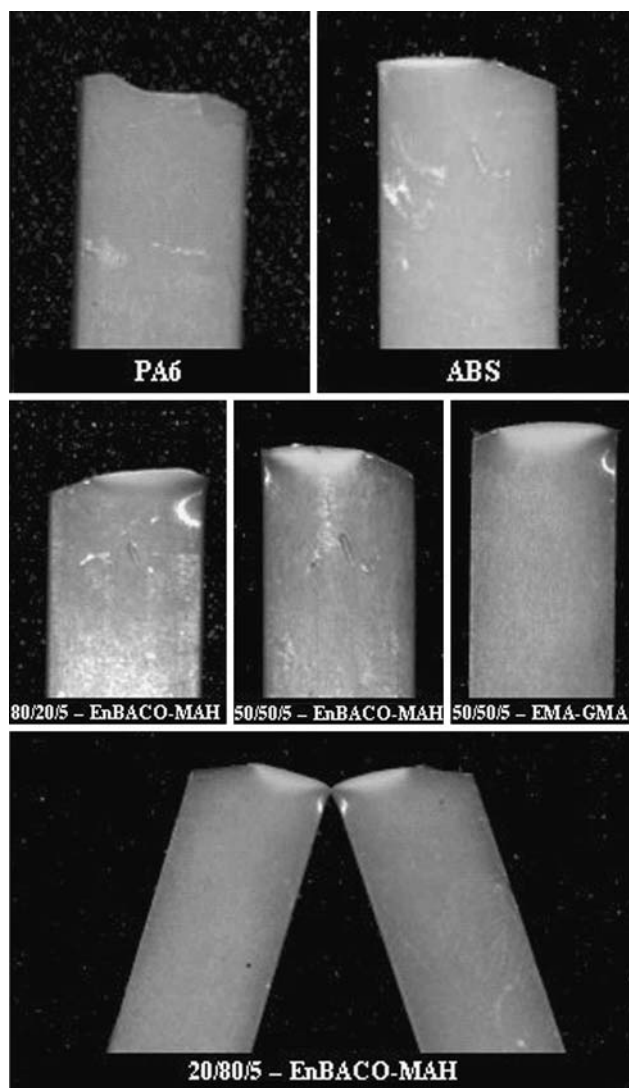


Fig. 7 Representative broken samples of PA6, ABS and compatibilized ABS/PA6 blends (The numbers correspond to ABS/PA6/Compatibilizer ratios)

Table 2 Impact-specific EWF values, average dispersed-phase particle size and Charpy impact strengths of materials

Material (ABS/PA6/Comp.)	Average dispersed-phase particle size [18, 19], (μ)	Essential work of fracture, w_e (kJ/m ²)	Non-essential work of fracture, βw_p (MJ/m ³)	Notched Charpy impact strength ASTM D 256 (kJ/m ²)
100/0/0	N/A	16.30	0.40	23.6
80/20/0	10.1	4.40	0.13	9.0
50/50/0	11.2	2.10	0.16	7.4
20/80/0	9.97	2.30	0.15	6.3
80/20/5- EnBACO-MAH	0.44	19.20	2.37	46.2
50/50/5- EnBACO-MAH	Co-continuous	25.10	2.64	58.0
20/80/5- EnBACO-MAH	0.86	21.10	2.22	55.9
80/20/5- EMA-GMA	1.04	17.90	1.64	25.9
50/50/5- EMA-GMA	Co-continuous	23.00	1.77	42.1
20/80/5- EMA-GMA	1.20	15.60	1.69	28.6
0/100/0	N/A	1.53	0.14	4.3

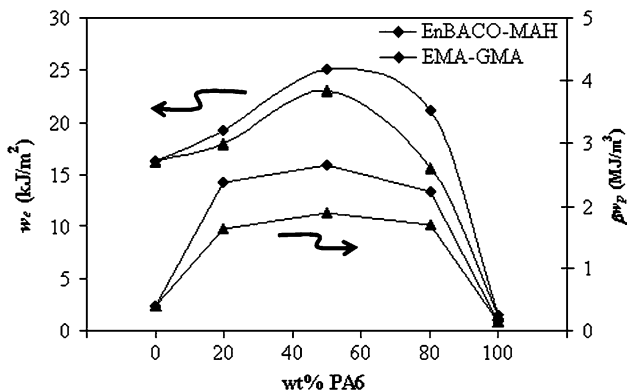


Fig. 8 w_e and βw_p versus PA6 content

particle can cavitate [34], therefore, larger rubber particles cavitate easier than smaller particles.

SEM micrograph of ABS, PA6 and incompatibilized 50ABS/50PA6 blend are shown in Fig. 9a–c. The fracture surface of ABS is smooth but tortuous. The magnified picture shows black holes left by cavitated rubbery phase of ABS. PA6’s fracture surface was smooth and includes large cracks indicating brittle fracture. The incompatibilized blends of ABS/PA6 fractured in brittle manner regardless of blend composition. This behaviour can be attributed to the too large size of the dispersed phases for effective toughening.

SEM micrographs of 80ABS/20PA6 blends compatibilized with 5% EnBACO-MAH and EMA-GMA are shown in Fig. 10. In these blends, ABS is continuous, whereas PA6 is dispersed phase. It is evident that the PA6 particles were pull-out from the ABS matrix. There is no deformation related to shear yielding that can be observed in the matrix phase, apparently due to the higher stiffness of PA6 particles.

The morphology of fracture surface of 50ABS/50PA6/5Comp. blend system (see Fig. 11) is different from that observed in 80ABS/20PA6. The failure is completely ductile. The fibrillar morphology probably obtained due to the massive shear yielding which is the energy absorbing mechanism. In the case of EMA-GMA, some micro-voids are seen between interconnected ligaments resulting in matrix tearing. However, in EnBACO-MAH, extend of fibrillation is much higher and the micro-voids are much smaller.

Microstructure of the 20ABS/80PA6/5Comp. blend system resembles traditional rubber-toughened polyamides (see Fig. 12). The predominant deformation mechanism in these materials is previously reported as rubber particle cavitation and subsequent matrix shear yielding [41, 42]. In the blends considered here, the black holes seen are the locations of rubber particles pulled-out from the matrix, which are surrounded by yielded polyamide ligaments. The shear yielding and particle pull-out co-exist both in EnBACO-MAH and EMA-GMA compatibilizers.

Conclusions

The impact fracture toughness of ABS/PA6 blends prepared at different ratios and compatibilized with CO modified ethylene-n butyl acrylate-maleic anhydride or ethylene-methyl acrylate-glycidyl methacrylate copolymers was examined by standard Charpy tests, EWF analysis and fracture surface morphologies. In EWF analysis, injection-moulded specimens were tested using pendulum impact tester as a function of the ligament length to determine the essential and non-essential work of fracture terms. The visual inspection of the specimens in which fracture was restrained indicates that crack propagated

Fig. 9 SEM micrographs of fracture surfaces of (a) ABS, (b) PA6 and (c) incompatibilized 50ABS/50PA6

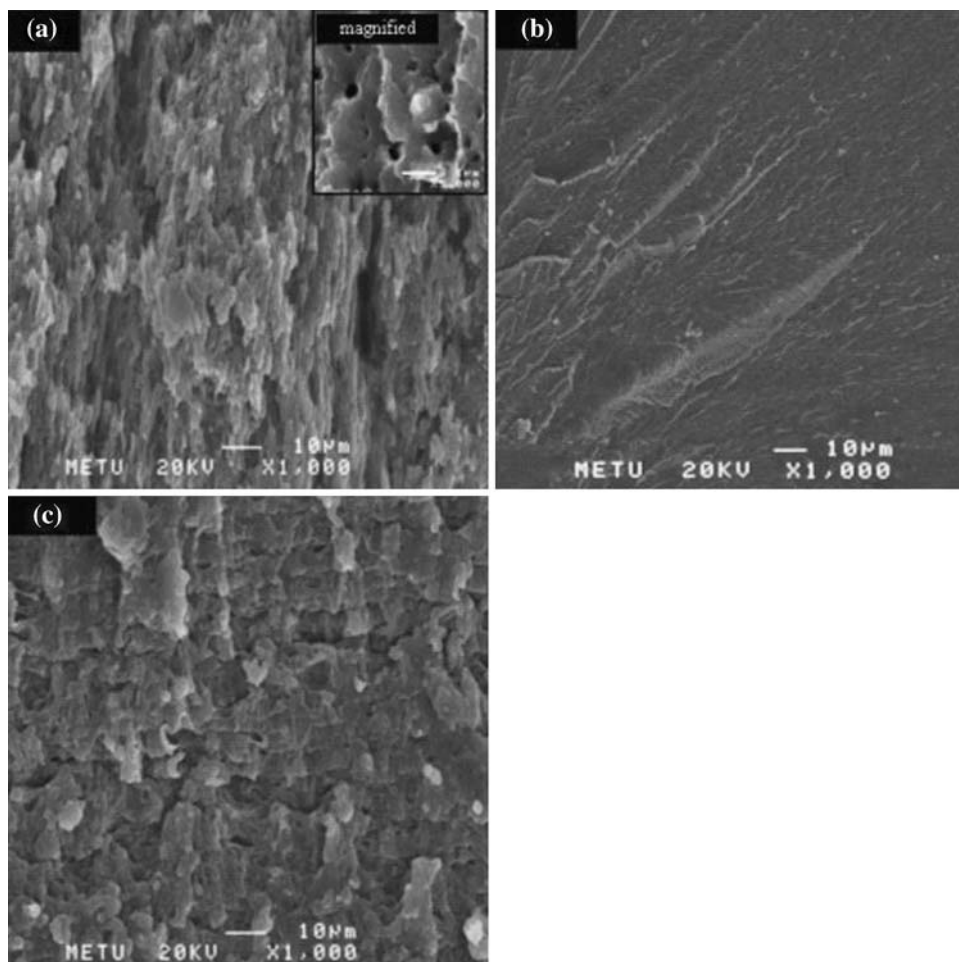
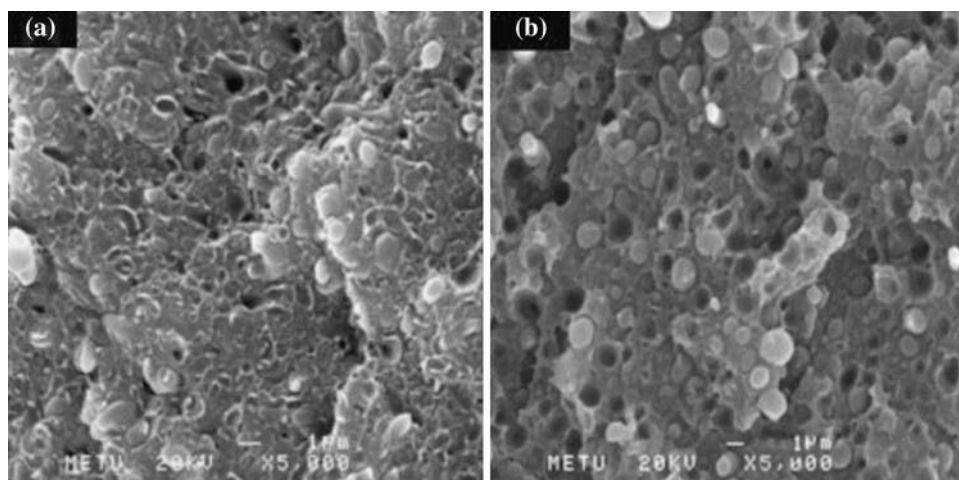


Fig. 10 SEM micrographs of fracture surfaces of (a) 80ABS/20PA6/5EnBACO-MAH, (b) 80ABS/20PA6/5EMA-GMA



before complete ligament yielding. Thus, yielding criterion is not satisfied. On the other hand, it is showed that the volume of the stress whitened zone is proportional to square of ligament length.

Despite the inconvenience in yielding criterion, EWF methodology is successfully employed in ABS/PA6/

Compatibilizer ternary blends. It is revealed from force versus displacement curves obtained from impact fracture tests that compatibilization of ABS/PA6 blends reduces the crack growth rate and increased the energy absorbed in the plastic region, so called stress whitened zone. The incompatibilized blends and neat-PA6 fracture in brittle manner,

Fig. 11 SEM micrographs of fracture surfaces of (a) 50ABS/50PA6/5EMA-GMA, (b) 50ABS/50PA6/5EnBACO-MAH

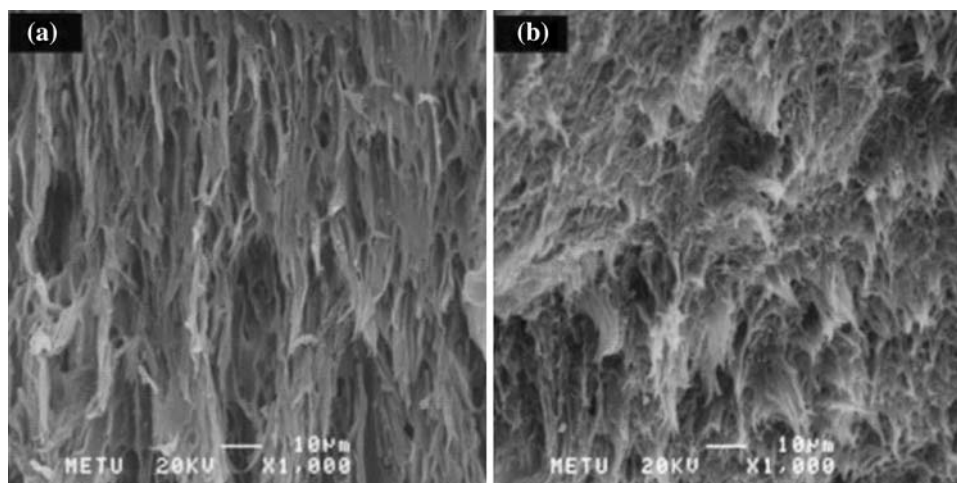
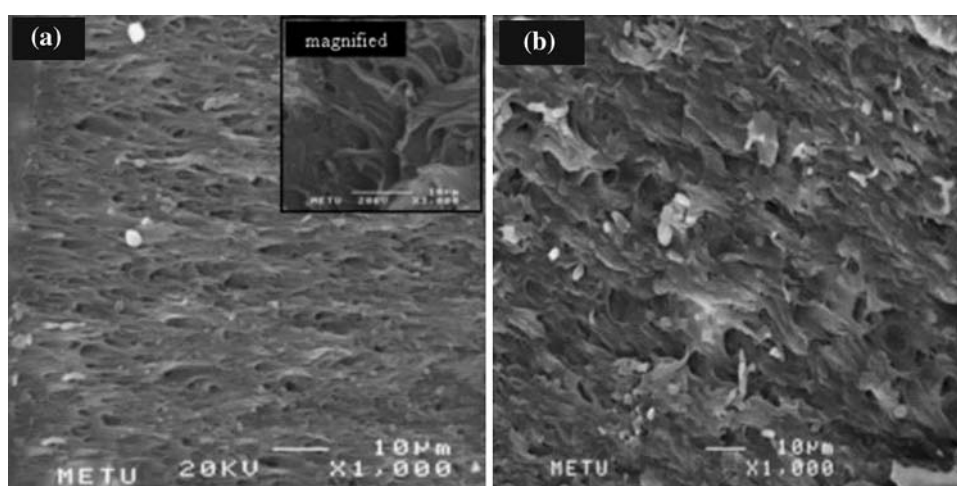


Fig. 12 SEM micrographs of fracture surfaces of (a) 20ABS/80PA6/5EnBACO-MAH, (b) 20ABS/80PA6/5-EMA-GMA



whereas compatibilized blends fracture in ductile manner. The essential work of fracture values increased with increasing PA6 in the blend up to 50ABS/50PA6/5Comp., give a maximum, and then dropped; on the contrary non-essential work of fracture values do not change much as a function of blend composition. The EWF values obtained in the case of EnBACO-MAH are higher than that of EMA-GMA regardless of blend composition. The trend of standard notched Charpy impact test is similar to that of essential work of fracture of blends.

The morphology of the fracture surfaces of ABS/PA6/Compatibilizer ternary blends exhibits variations with respect to blend composition. The main deformation in 80ABS/20PA6/5Comp. blends is the pull-out of the PA6 particles without shear yielding of the ABS matrix due to the higher stiffness of PA6 in comparison to ABS. The co-continuous blends of 50ABS/50PA6/5Comp. deform by forming fibrils occurring over a high fracture area. The deformation mechanism of the 20ABS/80PA6/5Comp. blends deduced from morphology of fracture surface look like the fracture mechanism of traditional rubber-

toughened polyamide. The type of deformation is cavitation of ABS particles followed by subsequent shear yielding of PA6.

References

1. Majumdar B, Keskkula H, Paul DR (1994) *Polymer* 35:5468
2. Majumdar B, Keskkula H, Paul DR (1994) *Polymer* 35:3164
3. Kudva RA, Keskkula H, Paul DR (2000) *Polymer* 41:225
4. Kudva RA, Keskkula H, Paul DR (2000) *Polymer* 41:239
5. Kitayama N, Keskkula H, Paul DR (2001) *Polymer* 42:3751
6. Chiu HT, Hsiao YK (2004) *Polym Eng Sci* 44:2340
7. Lee CW, Ryu SH, Kim HS (1997) *J Appl Polym Sci* 64:1595
8. Lai SM, Liao YC, Chen TW (2005) *Polym Eng Sci* 45:1461
9. Araujo EM, Hage JRE, Carvalho AJF (2004) *J Mat Sci* 39:1173
10. Gan PP, Paul DR (1994) *Polymer* 35:3513
11. Nishimoto M, Keskkula H, Paul DR (1989) *Polymer* 30:1279
12. Chu JP, Paul DR (1999) *Polymer* 40:2687
13. Kudva RA, Keskkula H, Paul DR (1998) *Polymer* 39:2447
14. Kayano Y, Keskkula H, Paul DR (1998) *Polymer* 39:2835
15. Mai YW, Powell P (1991) *J Polym Sci: Polym Phy* 29:785
16. Wu J, Mai YW (1996) *Polym Eng Sci* 36:2275
17. Wu J, Mai YW, Cotterell B (1993) *J Mater Sci* 28:3373
18. Ozkoc G, Bayram G, Bayramli E (2006) *J Appl Polym Sci* 104:924

19. Ozkoc G, Bayram G, Bayramli E (2006) In: Society of plastics engineering annual technical conference, Charlotte, NC
20. Mai YW, Cotterell B (1985) *Eng Fracture Mech* 21:123
21. Mai YW, Cotterell B (1986) *Int J Fracture* 32:105
22. Mai YW, Cotterell B, Horlyck R, Vigna G (1987) *Polym Eng Sci* 27:804
23. Test Protocol for Essential Work of Fracture (Version 5). European Structural Integrity Society (1997)
24. Fasce L, Bernal C, Frontini P, Mai YW (2001), *Polym Eng and Sci* 41:1
25. Wu J, Mai YW (1996) *Polym Eng Sci* 36:2275
26. Vu-Khanh T, de Charentenay FX (1985) *Polym Eng Sci* 25:841
27. Vu-Khanh T (1994) *Theor Appl Frac Mech* 21:83
28. Kudva RA, Keskkula H, Paul DR (2000) *Polymer* 41:335
29. Mai YW (1999) In: Paul DR, Bucknall CB (eds) *Polymer blends: formulation and performance*. Wiley
30. Sivaraman P, Chandrasekhar L, Mishra VS, Chakraborty BC, Varghese TO (2006) *Polymer Testing* 25:562
31. Huang JJ, Paul DR (2006) *Polymer* 47:3505
32. Borggreve RJM, Gaymans RJ, Schuijjer J, Housz JFI (1987) *Polymer* 28:1489
33. Margolina A, Wu S (1998) *Polymer* 29:2170
34. Bucknall CB (1997) *Toughened plastics*. Applied Science Publishers Ltd
35. Ben Jar P-Y, Wu RY, Kuboki T, Takahashi K, Shinmura T (1997) *J Mater Sci Let* 18:1489
36. Castellani L, Frassine R, Pavan A, Rink M (1996) *Polymer* 37:1329
37. Bernal CR, Frontini PF, Sforza M, Bibbo MA (1995) *J Appl Polym Sci* 58:1
38. Lazzeri A, Bucknall CB (1995) *Polymer* 36:2895
39. Sue HJ (1992) *J Mat Sci* 27:3098
40. Laura DM, Keskkula H, Barlow JW, Paul DR (2003) *Polymer* 44:3347
41. Sue HJ, Yee AF (1991) *J Mat Sci* 26:3449
42. Wong SC, Mai YW (2000) *Polymer* 41:5471